

Small- q Anomaly in the Dielectric Function and High-Temperature Oscillations of Screening Potential in 2D Electron Gas with Spin-Orbit Coupling

Guang-Hong Chen and M. E. Raikh

Department of Physics, University of Utah, Salt Lake City, Utah 84112

Abstract

We study the static dielectric function $\varepsilon(q)$ of 2D electron system with spin-orbit coupling in the frame of the random phase approximation. We demonstrate that, in addition to the well-known $2k_F$ -Kohn anomaly, spin-orbit coupling gives rise to the novel anomaly in the dielectric function at small $q = q_0 \ll k_F$, where q_0 is the distance between two Fermi surfaces. As a result of this anomaly a large-distance behavior of the potential from a point charge exhibits (in addition to the conventional Friedel oscillations) novel oscillations with a period $2\pi/q_0$. The remarkable feature of these oscillations is that they are not smeared out by the temperature. We show that the small- q anomaly also modifies the indirect exchange interaction of localized magnetic moments (RKKY interaction). In the presence of spin-orbit coupling this interaction acquires a high-temperature component.

PACS number(s): 71.45. Gm, 73.20-r, 73.20.Dx

I. INTRODUCTION

The dielectric function of a two-dimensional electron system was first evaluated by F. Stern [1] within the random phase approximation (RPA). In the static case, Stern obtained the following expression for $\varepsilon(q)$

$$\varepsilon(q) = \varepsilon_0(1 - v(q)F(q)), \quad (1)$$

where q is the wave vector and $v(q) = 2\pi e^2/\varepsilon_0 q$ is the Fourier component of the Coulomb interaction, ε_0 is the dielectric constant of the medium. The response function $F(q)$ is given by

$$F(q) = -\nu \quad (q \leq 2k_F) \quad (2)$$

$$F(q) = -\frac{\nu}{q}(q - \sqrt{q^2 - 4k_F^2}) \quad (q > 2k_F), \quad (3)$$

where $\nu = m^*/\pi\hbar^2$ is the 2D density of states; m^* is the effective mass. It is well-known that the singularity in $F(q)$ at $q = 2k_F$ leads to the Friedel oscillations of the screening potential. For a point charge at a distance d from a 2D plane the oscillatory part of the potential has the form

$$V_{osc}(\rho) = -\left(\frac{2e^2}{\varepsilon_0 a_B}\right) \frac{\sin(2k_F\rho)}{(2k_F\rho)^2} e^{-2k_F d}, \quad (4)$$

where $a_B = \hbar^2\varepsilon_0/m^*e^2$ is the effective Bohr radius. Eq. (4) applies at large distances, $k_F\rho \gg 1$. The result (4) is derived for zero temperature $T = 0$. Obviously, the oscillations are smeared out as T increases. This effect amounts to an additional factor $A(u)$ in Eq. (4) defined as

$$A(u) = \frac{u}{\sinh(u)}, \quad (5)$$

where $u = \pi k_F\rho T/E_F$. It follows from Eq. (5) that the power-law decay of $V_{osc}(\rho)$ persists at finite temperature from $\rho \sim k_F^{-1}$ to $\rho \sim k_F^{-1}(E_F/T)$. At larger ρ a crossover to the exponential decay $\propto \exp(-2\pi k_F\rho T/E_F)$ takes place.

The expression for $V_{osc}(\rho)$ can be straightforwardly generalized to the case of two or more 2D subbands. This is because the size-quantization wave functions in the direction perpendicular to the plane are orthogonal, so that the inter-subband transitions are forbidden. In this case $V_{osc}(\rho)$ is described by the sum of the Friedel oscillations from each subband.

The same argument would apply in the presence of the Zeeman splitting if one neglects the orbital action of the magnetic field. In this case, the transitions between the branches of the spectrum with different spin projections are forbidden.

In the present paper we demonstrate that the situation is quite different in the presence of the spin-orbit (SO) coupling. With SO coupling, the electronic states are classified not by the spin orientation but by the *chirality*. Our main results are as follows: (i) SO coupling gives rise to a new type of oscillations in $V(\rho)$ which are caused by virtual transitions between the states with different chirality; (ii) the distinguishing feature of these oscillations is that they survive the increasing of temperature (not smeared out with the increasing T).

To account for SO coupling, we choose the simplest form of the SO interaction for 2D electron system [2]

$$\hat{H}_{SO} = \alpha \mathbf{k} \cdot (\boldsymbol{\sigma} \times \mathbf{n}), \quad (6)$$

where \mathbf{k} is the momentum, \mathbf{n} is the unit vector normal to the 2D plane, $\boldsymbol{\sigma} = (\sigma_1, \sigma_2, \sigma_3)$ are the Pauli matrices, and α is the SO coupling constant. With spin-orbit term Eq. (6) the splitted Fermi surfaces for a *given* 2D subband represents two circles with radii (see Fig. 1)

$$k_F^{(1)} = -\frac{q_0}{2} + \sqrt{\frac{q_0^2}{4} + \frac{2m^*E_F}{\hbar^2}} = k_F - \frac{q_0}{2} \quad (7)$$

$$k_F^{(2)} = \frac{q_0}{2} + \sqrt{\frac{q_0^2}{4} + \frac{2m^*E_F}{\hbar^2}} = k_F + \frac{q_0}{2}, \quad (8)$$

where k_F is related to the Fermi energy as

$$k_F = \sqrt{\frac{q_0^2}{4} + \frac{2m^*E_F}{\hbar^2}}, \quad (9)$$

and $q_0 = k_F^{(2)} - k_F^{(1)}$ is expressed through the SO coupling constant as follows

$$q_0 = \frac{2m^*\alpha}{\hbar^2}. \quad (10)$$

It is important that the difference $k_F^{(2)} - k_F^{(1)}$ does not depend on the position of the Fermi level.

Our main observation is that, in contrast to the case of *different* 2D subbands, the virtual transitions between SO-split states within the *same* subband are allowed and, thus, *do contribute* to the response function. Below we will demonstrate that this contribution is singular at $q = q_0$. This singularity results in the following oscillatory behavior of the screening potential

$$V_{SO}(\rho) = -\left(\frac{2e^2}{\varepsilon_0 a_B}\right) \left(\frac{q_0}{2k_F}\right)^2 \frac{\cos(q_0 \rho)}{(q_0 \rho)^2}. \quad (11)$$

Comparing (11) to (4), one can see that the SO-induced oscillations do not contain the factor $\exp(-2k_F d)$. Strictly speaking, this factor should be replaced by $\exp(-q_0 d)$ in Eq. (11), but we assume throughout this paper that SO coupling is weak, i.e. $q_0 \ll k_F$. The magnitudes of the oscillations Eq. (11) and Eq. (4) are of the same order for $d = 0$. However, at elevated temperatures, V_{SO} will always dominate since the conventional Friedel oscillations get damped.

It is interesting to note that as far as the conventional Friedel oscillations are concerned, there is also a difference between the case of two size-quantization and two SO-split subbands. In the former case the large- ρ behavior of the screened potential is $V(\rho) \propto (\sin(2k_F^{(1)} \rho) + \sin(2k_F^{(2)} \rho))/\rho^2$, whereas in the latter case, as we will demonstrate below, these oscillations have the form $V(\rho) \propto (\sin(k_F^{(1)} + k_F^{(2)})\rho)/\rho^2$.

The paper is organized as follows: In Sec. II we evaluate the dielectric function $\varepsilon(q)$ for different domains of wave vector q . The spatial oscillations of the screened potential are studied in Sec. III. Concluding remarks are given in the Sec. IV.

II. DIELECTRIC FUNCTION WITH SO COUPLING

A. Spectrum and Eigenfunctions

With SO term Eq. (6), the Hamiltonian of a free electron has the form

$$H = \frac{\hbar^2 k^2}{2m} + \alpha \mathbf{k} \cdot (\boldsymbol{\sigma} \times \mathbf{n}). \quad (12)$$

The energy spectrum and the wave functions are given by

$$E_\mu(k) = \frac{\hbar^2 k^2}{2m} - \mu \alpha k \quad (13)$$

$$\chi_{\mathbf{k}\mu} = \frac{1}{\sqrt{2}} \begin{bmatrix} i\mu e^{-i\phi_{\mathbf{k}}} \\ 1 \end{bmatrix}, \quad \Psi_{\mathbf{k},\mu}(\boldsymbol{\rho}) = \frac{1}{\sqrt{A}} e^{i\mathbf{k}\cdot\boldsymbol{\rho}} \chi_{\mathbf{k}\mu}. \quad (14)$$

Here $\mu = \pm 1$ is the chirality, A is the normalization area, and $\phi_{\mathbf{k}}$ is the azimuthal angle of the vector \mathbf{k} .

B. General Formula for the Dielectric Function

We start with the RPA formula for $\varepsilon(q)$ applied to the case when free electron wave functions are the eigenfunctions of the Hamiltonian Eq. (12)

$$\frac{\varepsilon(q)}{\varepsilon_0} = 1 - v(q) \sum_{\mathbf{k},\mu,\mu'} |\chi_{\mathbf{k},\mu}^\dagger \chi_{\mathbf{k}+\mathbf{q},\mu'}|^2 \frac{n(E_\mu(k)) - n(E_{\mu'}(|\mathbf{k} + \mathbf{q}|))}{E_\mu(k) - E_{\mu'}(|\mathbf{k} + \mathbf{q}|)}, \quad (15)$$

where $n(E_\mu(k))$ is the Fermi-Dirac distribution function, and

$$|\chi_{\mathbf{k},\mu}^\dagger \chi_{\mathbf{k}+\mathbf{q},\mu'}|^2 = \frac{1}{2} (1 + \mu\mu' \cos(\phi_{\mathbf{k}+\mathbf{q}} - \phi_{\mathbf{k}})), \quad (16)$$

are the overlap integrals. It is important to note that the virtual transitions between different chiralities are *allowed*. In the case of two size-quantization subbands, the overlap integral would *reduce to the Kronecker symbol*, so that $\varepsilon(q)$ would represent a sum of contributions from each subband. In contrast, as it follows from Eq. (16), the overlap integral vanishes for $\mu \neq \mu'$ *only if* $\mathbf{k} \parallel \mathbf{q}$.

In evaluating the dielectric function, it is convenient first to perform the angular integration by introducing the auxiliary variable in Eq. (15)

$$\begin{aligned}
\frac{\varepsilon(q)}{\varepsilon_0} &= 1 - \frac{v(q)}{4\pi^2} \sum_{\mu, \mu'} \int_0^\infty dk k \int_0^\infty dp p \int_0^{2\pi} d\phi_{\mathbf{k}} \left(1 + \mu\mu' \frac{\mathbf{k} \cdot (\mathbf{k} + \mathbf{q})}{kp} \right) \times \\
&\quad \left(\frac{n(E_\mu(k)) - n(E_{\mu'}(p))}{E_\mu(k) - E_{\mu'}(p)} \right) \delta(p^2 - |\mathbf{k} + \mathbf{q}|^2) \\
&= 1 - v(q) \sum_{\mu, \mu'} F_{\mu\mu'}(q),
\end{aligned} \tag{17}$$

where we introduced the following notation

$$\begin{aligned}
F_{\mu\mu'}(q) &= \frac{1}{4\pi^2} \int dk k \int dp p \int d\phi_{\mathbf{k}} \left[1 + \mu\mu' \frac{\mathbf{k} \cdot (\mathbf{k} + \mathbf{q})}{kp} \right] \times \\
&\quad \left[\frac{n(E_\mu(k)) - n(E_{\mu'}(p))}{E_\mu(k) - E_{\mu'}(p)} \right] \delta(p^2 - |\mathbf{k} + \mathbf{q}|^2).
\end{aligned} \tag{18}$$

Integrating over $\phi_{\mathbf{k}}$, we obtain

$$F_{\mu\mu'}(q) = \frac{1}{4\pi^2} \int dk \int dp \frac{n(E_\mu(k)) - n(E_{\mu'}(p))}{E_\mu(k) - E_{\mu'}(p)} \left(\frac{q^2 - (k-p)^2}{(k+p)^2 - q^2} \right)^{-\frac{\mu\mu'}{2}}. \tag{19}$$

It immediately follows from symmetry that $F_{1,-1} = F_{-1,1}$. The further calculations are different for the cases $\mu = \mu'$ and $\mu = -\mu'$. In the next subsections we consider these cases separately.

C. The case $\mu = -\mu'$

The expression for $F_{1,-1}(q)$ can be conveniently rewritten in the form

$$F_{1,-1}(q) = \frac{\nu}{2\pi} \int_0^\infty dk [n(E_{+1}(k))G_+(k, q) + n(E_{-1}(k))G_-(k, q)], \tag{20}$$

where the function $G_\pm(k, q)$ is defined as

$$G_\pm(k, q) = \int_0^\infty \frac{dp}{(k+p)(k-p \pm q_0)} \sqrt{\frac{q^2 - (k-p)^2}{(k+p)^2 - q^2}}. \tag{21}$$

It is presumed that the integrand is zero when the expression under the square root is negative.

Consider now the case of small $q \ll k_F$. Then the actual limits of integration in Eq. (21) are $(k-q, k+q)$, i.e. p is close to k . This allows to evaluate Eq. (21) analytically

$$G_{\pm}(k, q) \approx \frac{1}{4k^2} \int_{k-q}^{k+q} dp \frac{\sqrt{q^2 - (k-p)^2}}{k-p \pm q_0} = \pm \frac{\pi}{4k^2} \left[q_0 - \sqrt{q_0^2 - q^2} \theta(q_0 - q) \right], \quad (22)$$

where $\theta(x)$ is a step-function.

We see that in the small- q limit, the q and k dependencies in the $G(k, q)$ get decoupled from each other so that the q -dependence of the response function $F_{1,-1}(q)$ is the same as the q -dependence of Eq. (22):

$$F_{1,-1}(q) = \frac{\nu}{8} \left[q_0 - \sqrt{q_0^2 - q^2} \theta(q_0 - q) \right] \int_0^{\infty} dk \frac{n(E_{+1}(k)) - n(E_{-1}(k))}{k^2} \quad (23)$$

First, we realize that the response function exhibits a square root singularity at $q = q_0$. This singularity is depicted schematically in Fig. 2a. The second important observation is that, since q_0 is determined by the parameters of the electron spectrum and does not depend on the Fermi level position (see Eq. (10)), the temperature dependence of $F_{1,-1}(q)$ is very weak. Indeed, the straightforward calculation of the integral over k yields

$$F_{1,-1}(q, T) = -\frac{\nu q_0}{8k_F^2} \left[q_0 - \sqrt{q_0^2 - q^2} \theta(q_0 - q) \right] \left[1 + \frac{\pi^2}{6} \left(\frac{T}{E_F} \right)^2 \right]. \quad (24)$$

Such temperature dependence should be contrasted to that of the conventional $2k_F$ -anomaly. At finite T , the anomalous term, $\sqrt{q^2 - 4k_F^2}$, in Eq. (3) is replaced by [3,4]

$$\frac{1}{2} \int dx \frac{\sqrt{q^2 - 4k_F^2 + 8m^*Tx/\hbar^2}}{\cosh^2 x}, \quad (25)$$

which leads to the smearing of the anomaly within the region $|q - 2k_F| \sim k_F T / E_F$.

Let us consider the case of large $q \sim (k_F^{(1)} + k_F^{(2)}) = 2k_F$. In this case the limits of the integration in Eq. (21) are $(q-k, \infty)$. By noting that the main contribution to the anomaly comes from the vicinity of $q \sim (k+p)$, the integral can be simplified as

$$G_{\pm}(k, q) \approx \frac{1}{\sqrt{2q}} \int_{q-k}^{\infty} \frac{dp}{(k-p \pm q_0) \sqrt{k+p-q}} = -\frac{\pi}{\sqrt{2q}} \frac{\theta(q - 2k \mp q_0)}{\sqrt{q - 2k \mp q_0}}, \quad (26)$$

Substituting Eq. (26) into Eq. (20) leads to the following results for the response function

$$F_{1,-1}(q) = -\frac{\nu}{\sqrt{2}}, \quad \text{for } q < 2k_F \quad (27)$$

$$F_{1,-1}(q) = -\frac{\nu}{\sqrt{2}} \left(1 - \sqrt{\frac{q}{2k_F} - 1} \right), \quad \text{for } q \geq 2k_F. \quad (28)$$

Eqs. (27) and (28) apply in the domain $q - 2k_F \ll k_F$. We conclude that the anomaly occurs at $q = k_F^{(1)} + k_F^{(2)} = 2k_F$. This should be contrasted to the anomalies coming from the terms with $\mu = \mu'$ in Eq. (15) (intrasubband transitions). These anomalies are studied in the next subsection.

D. The case $\mu = \mu'$

In this case the anomalies occur at $q = 2k_F^{(1)}$ in $F_{1,1}(q)$ and at $q = 2k_F^{(2)}$ in $F_{-1,-1}(q)$. To extract the non-analytic behavior, we note that the main contribution to the integral Eq. (19) comes from $k, p \sim k_F$ and $q \sim k + p$, so that we can simplify the expression for $F_{1,1}(q)$ and $F_{-1,-1}(q)$ in the following way

$$F_{1,1}(q) = \frac{\sqrt{2}\nu}{\pi\sqrt{q}(q+q_0)} \int \int dkdp \frac{n(E_{+1}(k))\sqrt{k+p-q}}{k-p}, \quad (29)$$

$$F_{-1,-1}(q) = \frac{\sqrt{2}\nu}{\pi\sqrt{q}(q-q_0)} \int \int dkdp \frac{n(E_{-1}(k))\sqrt{k+p-q}}{k-p}. \quad (30)$$

Then by straightforward calculation we get

$$F_{1,1}(q) = F_{-1,-1}(q) = \frac{\sqrt{2}\nu}{3} \quad \text{for } q < 2k_F^{(1,2)}, \quad (31)$$

$$F_{1,1}(q) = \frac{\sqrt{2}\nu}{3} \left[1 - \left(\frac{q - 2k_F^{(1)}}{2k_F^{(1)}} \right)^{3/2} \right], \quad \text{for } q \geq 2k_F^{(1)}, \quad (32)$$

$$F_{-1,-1}(q) = \frac{\sqrt{2}\nu}{3} \left[1 - \left(\frac{q - 2k_F^{(2)}}{2k_F^{(2)}} \right)^{3/2} \right] \quad \text{for } q \geq 2k_F^{(2)}. \quad (33)$$

We see that instead of conventional $\sqrt{q - 2k_F}$ anomaly, we obtained much weaker anomalies $\propto \left(q - 2k_F^{(1,2)} \right)^{3/2}$. The origin of such a weakening is that for virtual transitions, $k_F^{(1,2)} - 2q \rightarrow -k_F^{(1,2)}$, which give rise to the conventional Kohn anomaly, the corresponding overlap integral, Eq. (16), is identically zero in the presence of the SO coupling.

III. OSCILLATIONS OF THE SCREENING POTENTIAL

Consider a point charge e at distance d from the 2D plane. The potential created by this charge within the plane is given by [3]

$$V(\rho) = e \int_0^\infty dq \frac{e^{-qd} J_0(q\rho)}{\varepsilon(q)}. \quad (34)$$

As we demonstrated in the previous section, the dielectric function $\varepsilon(q)$ exhibits anomalous behavior at small $q = q_0$ and also at $q = k_F^{(1)} + k_F^{(2)}$. Besides, there are weak anomalies at $q = 2k_F^{(1)}$, $q = 2k_F^{(2)}$ caused by the intrasubband virtual transitions.

The general approach for extracting the oscillating behavior of $V(\rho)$ is as follows. Suppose that $\varepsilon(q)$ has an anomaly at some $q = q_c$. Then the integrand in Eq. (34) should be expanded with respect to $\delta\mathcal{F}$ defined as

$$\delta\mathcal{F}(\kappa) = F(q_c + \kappa) - F(q_c), \quad (35)$$

and the Bessel function should be replaced by its large- ρ asymptotics. This leads to the following general formula for the oscillating part of $V(\rho)$

$$V(\rho) = \frac{ev(q_c)}{\varepsilon_0} \sqrt{\frac{2}{\pi q_c \rho}} \left[\cos(q_c \rho - \frac{\pi}{4}) I_1 - \sin(q_c \rho - \frac{\pi}{4}) I_2 \right] \exp(-q_c d), \quad (36)$$

where the integrals I_1, I_2 are defined as

$$I_1 = \int d\kappa \delta\mathcal{F}(\kappa) \cos(\kappa\rho), \quad (37)$$

$$I_2 = \int d\kappa \delta\mathcal{F}(\kappa) \sin(\kappa\rho). \quad (38)$$

By using the results obtained in the previous sections, we can now easily carry out the calculations (Eq. (36)- Eq. (38)).

(i) For anomaly at $q_c = q_0$, we have

$$\delta\mathcal{F}(\kappa) \approx \frac{\sqrt{2\nu} q_0^{3/2}}{8 k_F^2} \sqrt{-\kappa} \quad (39)$$

and $\varepsilon(q_c) \approx \varepsilon_0$. This leads us to the spin-orbit oscillations Eq. (11).

(ii) For anomaly at $q_c = k_F^{(1)} + k_F^{(2)} = 2k_F$, the form of $\delta\mathcal{F}$ was shown to be

$$\delta\mathcal{F}(\kappa) = \nu \sqrt{\frac{\kappa}{k_F}}, \quad (40)$$

where we have considered the contribution of the $F_{-1,1}(q)$ which gives the same contribution as $F_{1,-1}(q)$. It is worth noting that this form coincides with the standard form of the Kohn anomaly in 2D. Thus for the oscillations with period π/k_F we get the same form of the screening potential as Eq. (4).

(iii) At $q_c = 2k_F^{(1,2)}$, it follows from Eqs. (32) and (33) that

$$\delta\mathcal{F}(\kappa) = \frac{\nu}{3} \left(\frac{\kappa}{2k_F^{(1,2)}} \right)^{3/2}. \quad (41)$$

Substituting this form into Eqs. (36-38) results in

$$V_{osc}(\rho) = \frac{3\sqrt{2}e^2}{2\varepsilon_0 a_B} \frac{\sin(2k_F^{(1,2)}\rho)}{(2k_F^{(1,2)}\rho)^3} e^{-2k_F^{(1,2)}d}. \quad (42)$$

We see that oscillations with “usual” periods $\pi/k_F^{(1,2)}$ fall off as $1/\rho^3$, i.e. faster than the conventional oscillations Eq. (4).

IV. CONCLUSION

The main result of the present paper is the prediction of the novel oscillations of the screening potential originating from the spin-orbit term in the Hamiltonian of a free electron. In our calculations we assumed that the bare energy spectrum is parabolic. We also assumed that the origin of the spin-orbit term is the asymmetry of the confinement potential [2] and neglected the term coming from the absence of the inversion symmetry in the bulk [5]. Note, however, that if the Dresselhaus mechanism [5] dominates the SO coupling (in this case $\hat{H}_{SO} \propto (\sigma_x k_x - \sigma_y k_y)$), the results of the present paper remain unchanged.

There are two cases when the spin-orbit-induced oscillations, studied in the present paper, dominate over the conventional $2k_F$ -oscillations [1]. First, with increasing temperature, $2k_F$ -oscillations get damped, while q_0 -oscillations remain almost temperature-independent. This

situation is illustrated in Fig. 3. It is seen that for parameters of Fig. 3 the Friedel oscillations almost disappear at $T \approx 0.1E_F$. Second, with increasing the spacing d from the ionized impurity to the 2D electron plane the amplitude of the conventional oscillations falls off as $\exp(-2k_F d)$ [1], whereas for q_0 -oscillations this dependence is much weaker $\propto \exp(-q_0 d)$. Fig. 2 illustrates how the q_0 -oscillations take over as d is increased. Note, that large values of the spacing d is a necessary requirement for high mobility of 2D electron systems [6]. On the other hand, we considered the ideal electron gas, in the sense that we assumed the condition $q_0 l \gg 1$, l being the mean free path, to be met. Thus, the large values d is the domain of validity of our results.

Another application of the results obtained in the present paper is the effect of the SO coupling on indirect exchange interaction of localized magnetic moments (RKKY interaction). It is straightforward to generalize the expression for RKKY in two dimensions [7] to include the SO coupling

$$H_{RKKY}(\rho_{12}) = J^2 \left[\Phi_1(\rho_{12}) \mathbf{S}_1 \cdot \mathbf{S}_2 + (\Phi_2(\rho_{12}) - \Phi_1(\rho_{12})) (\mathbf{S}_1 \cdot \mathbf{n})(\mathbf{S}_2 \cdot \mathbf{n}) \right], \quad (43)$$

where ρ_{12} is the distance between the two localized spins \mathbf{S}_1 and \mathbf{S}_2 , J is the contact interaction constant, and the functions $\Phi_1(\rho)$, $\Phi_2(\rho)$ are defined as

$$\Phi_1(\rho) = \sum_{\mu\mu'} \int \frac{d^2 q}{(2\pi)^2} e^{i\mathbf{q}\cdot\rho} \Pi_{\mu\mu'}(q), \quad (44)$$

$$\Phi_2(\rho) = \sum_{\mu\mu'} \int \frac{d^2 q}{(2\pi)^2} e^{i\mathbf{q}\cdot\rho} F_{\mu\mu'}(q). \quad (45)$$

In Eq. (45) the response function $F_{\mu\mu'}(q)$ is defined by Eq. (18), whereas $\Pi_{\mu\mu'}(q)$ is the conventional polarizability

$$\Pi_{\mu\mu'}(q) = \sum_{\mathbf{k}} \frac{n(E_\mu(k)) - n(E_{\mu'}(|\mathbf{k} + \mathbf{q}|))}{E_\mu(k) - E_{\mu'}(|\mathbf{k} + \mathbf{q}|)}. \quad (46)$$

In the absence of the SO coupling we have $\Phi_1(\rho) = \Phi_2(\rho)$, and the interaction falls off at large distances as $\sin(2k_F \rho)/\rho^2$. As it was demonstrated above, with SO coupling the function $\Phi_1(\rho)$ contains high-temperature oscillations, $\cos(q_0 \rho)/\rho^2$ resulting from the

term $F_{1,-1}(q) = F_{-1,1}(q)$ in the r.h.s of Eq. (44). The function $\Phi_2(\rho)$ also exhibits high-temperature oscillations due to the term $\Pi_{1,-1}(q) = \Pi_{-1,1}(q)$ in the r.h.s of Eq. (45). The small- q anomaly in this term can be extracted in the similar way as it was done in Sec. II. We list only the final result

$$\Pi_{1,-1}(q) = \frac{\nu\theta(q_0 - q)}{4\sqrt{q_0^2 - q^2}}. \quad (47)$$

It is seen that the anomaly at $q = q_0$ in $\Pi_{1,-1}$ is much stronger than in $F_{1,-1}$. As a result, at large distances, $\Phi_2(\rho)$ is much bigger (by a factor $\sim k_F^2\rho/q_0$) than $\Phi_1(\rho)$. Then the ρ -dependence of the indirect exchange interaction takes the form $\sin(q_0\rho)/\rho$. As it follows from Eq. (43) the in-plane components of \mathbf{S}_1 and \mathbf{S}_2 interact at large ρ much stronger than the normal components.

As a final remark, we address the above assumption that the SO splitting of the Fermi surface does not depend on k_F . Strictly speaking, since k_F is determined by the electron concentration n , and, in turn, the change of n results in the change of the confinement potential, there should be a certain dependence of α on n . Recent magnetotransport experiments on different 2D electronic systems yield either α weakly changing with n (Refs. [8], [9]) or, α , roughly, inversely proportional to n (Ref. [10]). Meanwhile, it is important to note that α depends only on the *total* concentration of electrons, which does not depend on temperature. Thus, our main conclusion that spin-orbit-induced anomaly in $\varepsilon(q)$ is not smeared out by temperature is insensitive to the actual dependence $\alpha(n)$. This dependence can govern only the position of the anomaly.

Acknowledgements

The authors are strongly grateful to T. V. Shahbazyan for careful reading the manuscript and many valuable suggestions. We acknowledge the stimulating discussions with R. R. Du, E. I. Rashba, and Y. S. Wu. Discussions with H. U. Baranger and Y. Imry are also gratefully acknowledged. One of the authors (G.H.C.) thanks A. Galstyan for technical

assistance in preparation of the manuscript. M.E.R. is grateful to the Aspen Center for Physics for hospitality.

REFERENCES

- ¹ F. Stern, Phys. Rev. Lett, **18**, 546 (1967).
- ² Yu. A. Bychkov and E. I. Rashba, Pis'ma Zh. Eksp. Teor. Fiz. **39**, 64 (1984) [JETP Lett. **39**, 78 (1984)].
- ³ P. F. Maldague, Surf. Sci., **73**, 296 (1978).
- ⁴ T. Ando, A. B. Fowler and F. Stern, Rev. Mod. Phys., **54**, 437 (1982).
- ⁵ G. Dresselhaus, Phys. Rev., **100**, 580 (1955).
- ⁶ H. L. Störmer, Surf. Sci., **132**, 518 (1983).
- ⁷ C. Kittel, in *Solid State Physics*, edited by F. Seitz, D. Turnbull, and H. Ehrenreich (Academic, New York, 1968), Vol. 22, p. 1.
- ⁸ P. Ramvall, B. Kowalski, and P. Omling, Phys. Rev. B **55**, 7160 (1997).
- ⁹ J. P. Heida, B. J. van Wees, J. J. Kuipers, and T. M. Klapwijk, Phys. Rev. B **57**, 11911 (1998).
- ¹⁰ J. Nitta, T. Akazaki, and H. Takayanagi, Phys. Rev. Lett. **78**, 1335 (1997).

FIGURES

FIG. 1. The energy spectrum of a 2D system with spin-orbit coupling; upper and lower branches correspond to chiralities $\mu = -1$ and $\mu = 1$ respectively; the difference between two Fermi momenta $k_F^{(2)}$ and $k_F^{(1)}$ is q_0 determined by Eq. (10).

FIG. 2. The numerical results for large- ρ behavior of dimensionless screened potential $V(\rho)(\frac{4e^2}{\epsilon_0 a_B})^{-1}$ at $T = 0$ are plotted for different distances, d , of a point charge from the 2D plane at $q_0/2k_F = 1/4$. (a) $d = a_B$. The solid curve represents the result calculated within the Thomas-Fermi approximation: $\epsilon(q) = \epsilon_0(1+2/qa_B)$. Dotted curve is the RPA result in the absence of the SO coupling featuring the Friedel oscillations. Dashed-dotted curve is plotted with $F(q)$ in the form of Eq. (23) and features the q_0 -oscillations. The inset shows schematically the small- q anomaly in the response function $F(q)$. (b) the same as (a) for $d = 1.5a_B$. (c) the oscillating parts of the screened potential for $d = a_B$ and $d = 1.5a_B$. Dotted and dashed-double dotted curves correspond to the Friedel oscillations. Thick solid and thick dashed-dotted curves correspond to the q_0 -oscillations.

FIG. 3. Asymptotics of the screened potential $V(\rho)$ in the units of $2e^2/\epsilon_0 a_B$ are plotted at different temperatures at $q_0/2k_F = 1/4$. Dotted and solid curves show the $2k_F$ -oscillations at $T = 0$ and $T = 0.1E_F$ respectively. Thick curve represents the q_0 -oscillations, Eq. (11), their change with temperature from $T = 0$ to $T = 0.1E_F$ being smaller than the thickness of the curve.

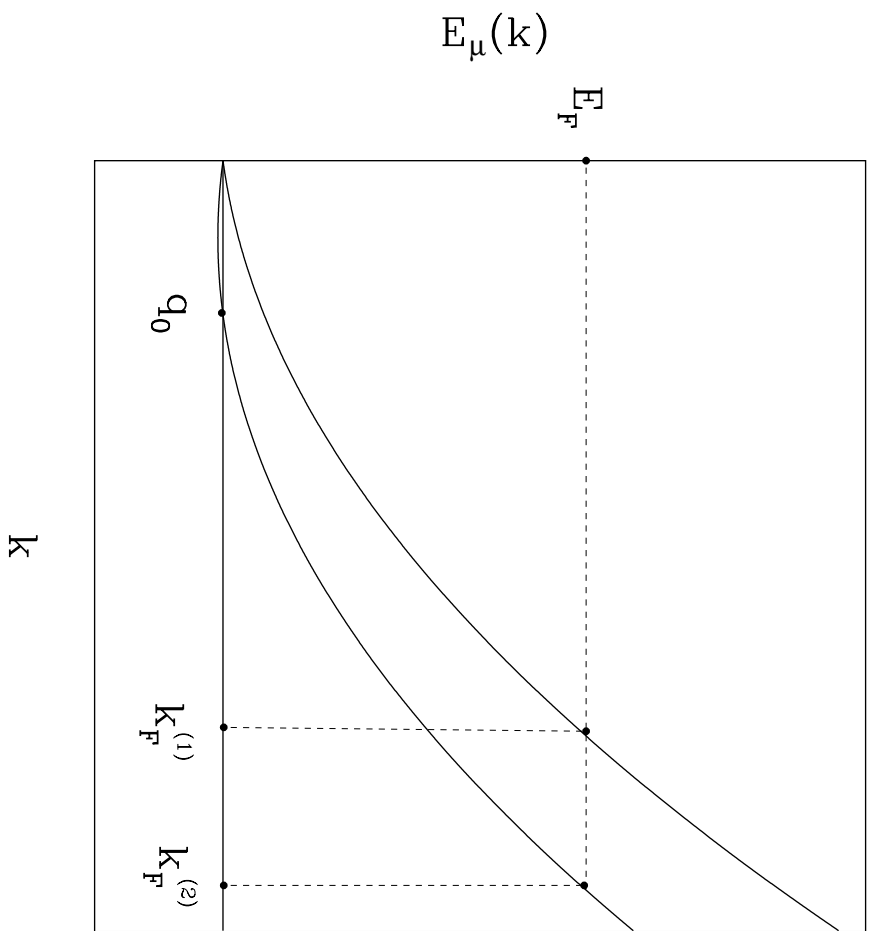


Fig. 1

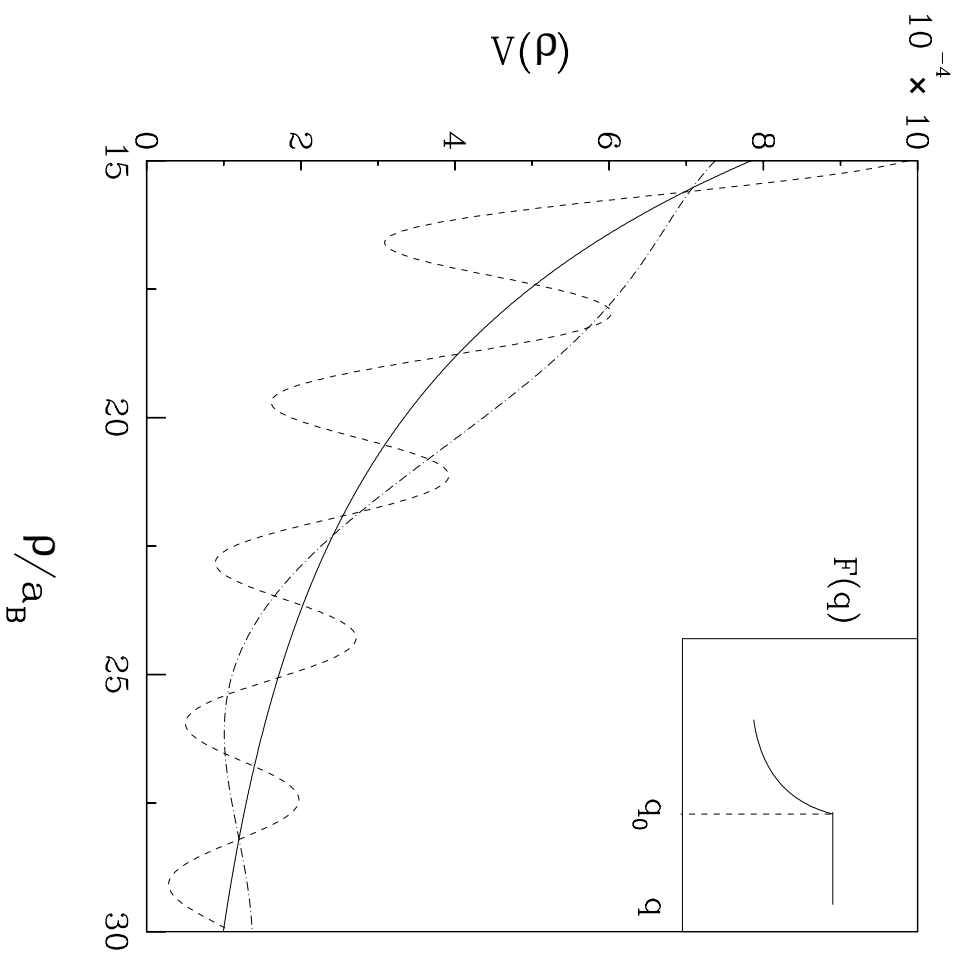


Fig. 2a

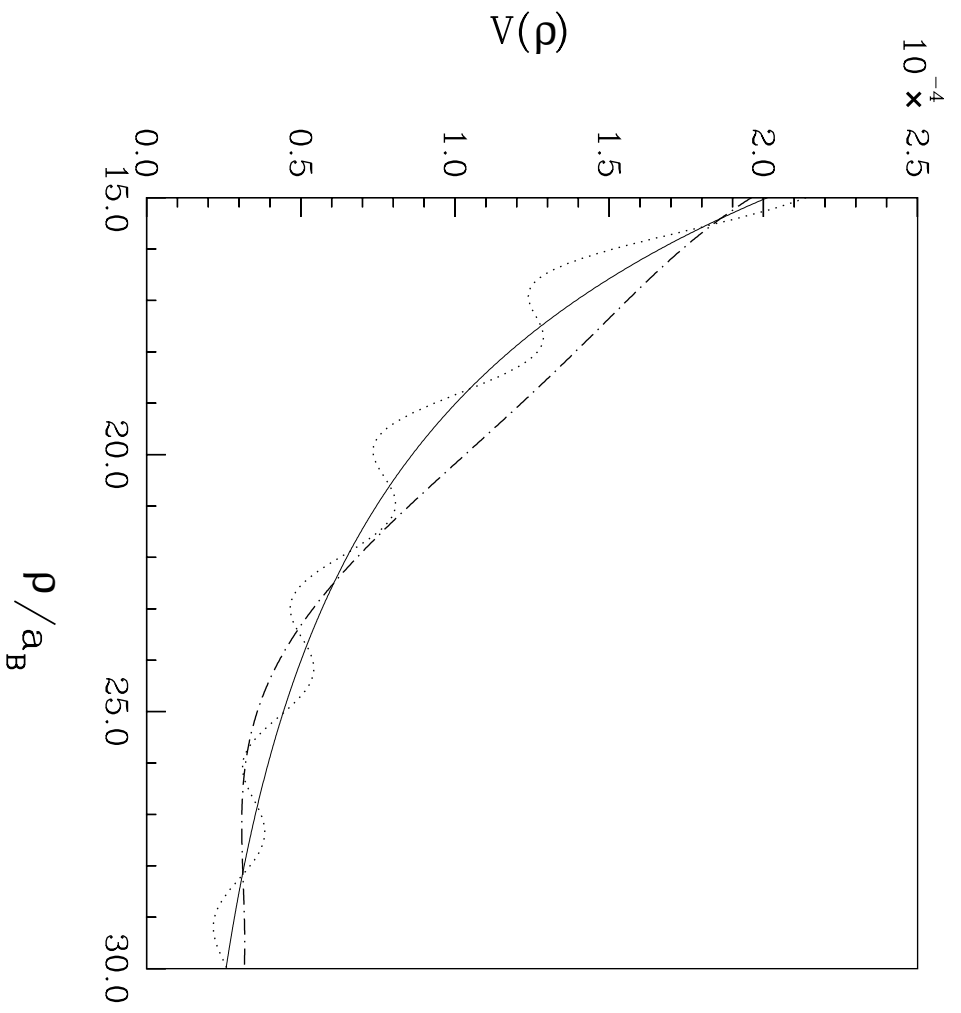


Fig.2b

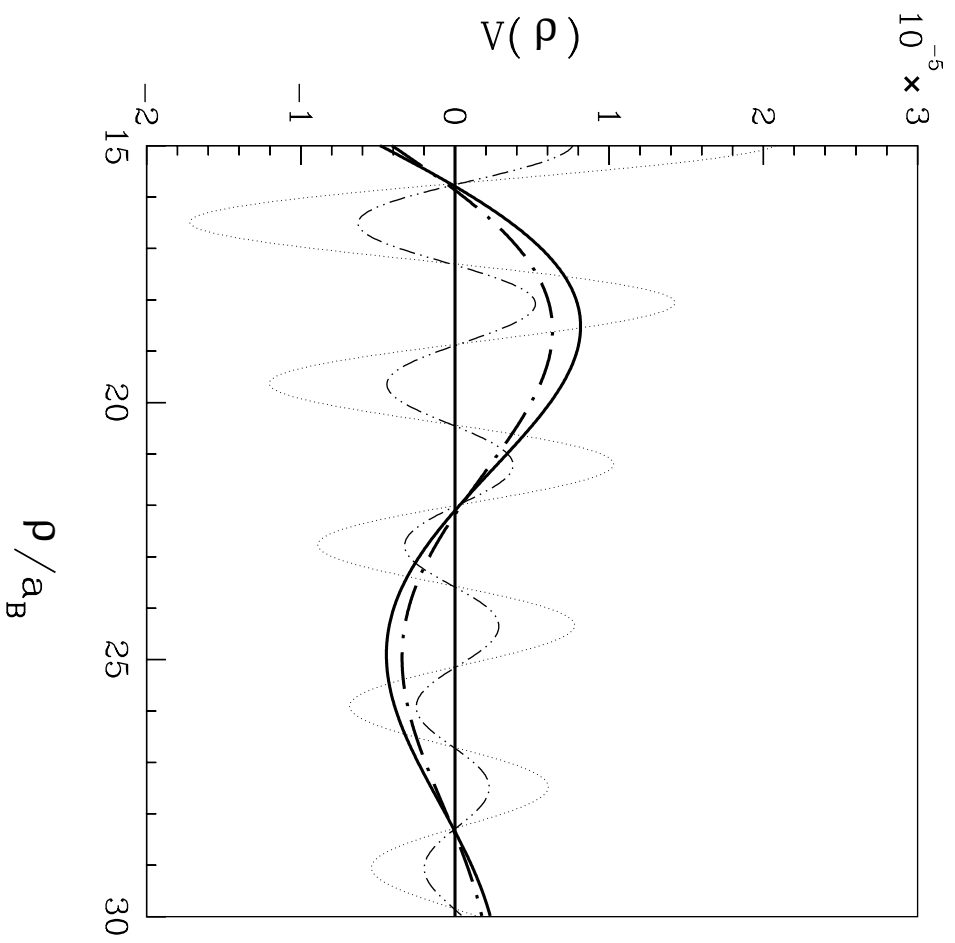


Fig. 2c

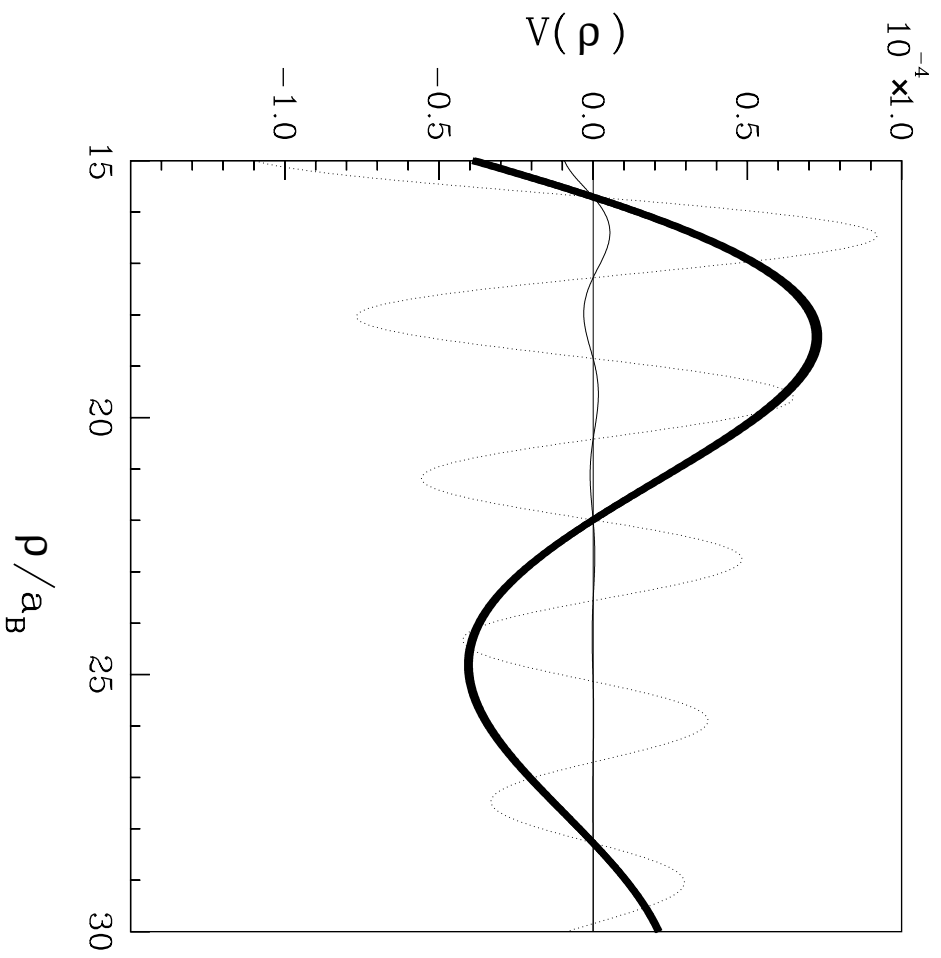


Fig. 3